Supporting Information

Macrocyclization of the ATCUN motif controls metal binding and catalysis

Kosh P. Neupane, Amanda R. Aldous and Joshua A. Kritzer*

Department of Chemistry, Tufts University, 62 Talbot Avenue, Medford, MA 02155, United States

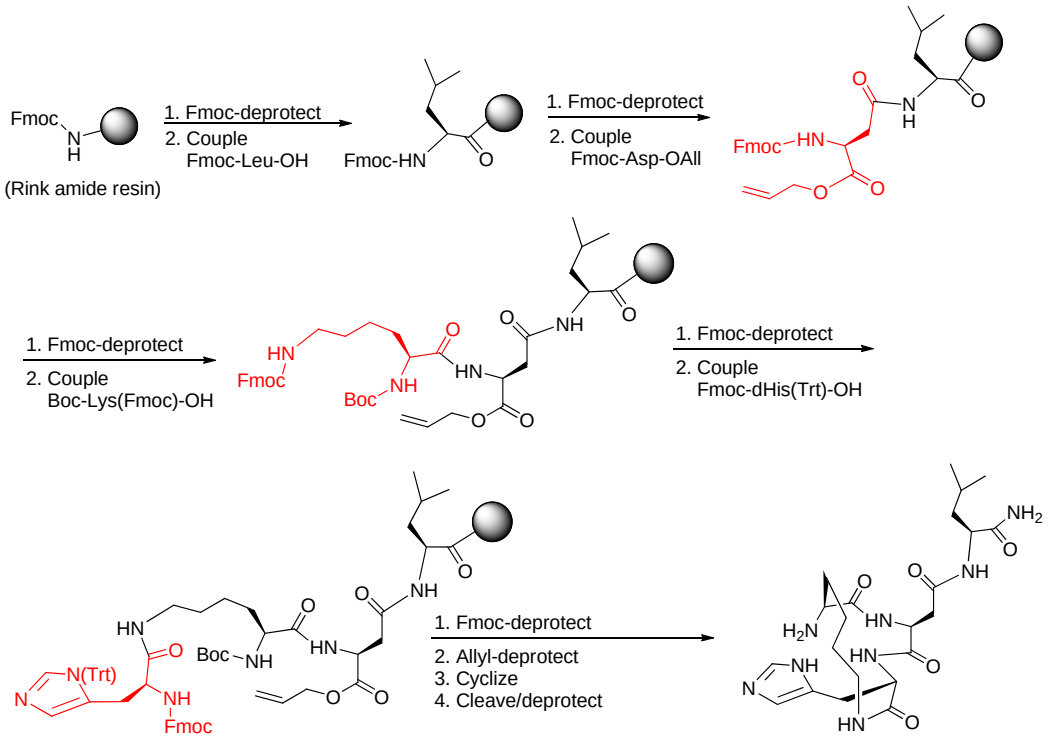

Scheme 1. Synthesis scheme for cyclic peptide **1**. Cyclic peptides **2** and **3** were synthesized in an analogous manner. Further synthesis details for peptides **1-6** are described in the Methods section of the main text.

Table S1. Characterization of Peptides by HPLC and Mass Spec

Peptide Sequence	Retention Time (HPLC)		ESI Mass/MALDI		Overall % Yield
	Analytical C18	Preparative C8	Calc.	Found	(after HPLC)
cyclo$^{1\text{-}3}$[Lys-Asp(Leu)-DHis], **1**	9.5	7.6	492.59	493.36	20
cyclo$^{1\text{-}3}$[DLys-Asp(Leu)-His], **2**	9.8	7.5	492.59	493.45	17
cyclo$^{1\text{-}3}$[Lys-Asp(Leu)-His], **3**	9.2	6.7	492.59	493.27	19
NH_2-Gly-Gly-His-Leu-$CONH_2$, **4**	9.0	6.5	381.43	381.01	60
NH_2-Gly-Gly-DHis-Leu-$CONH_2$, **5**	8.7	6.5	381.43	382.67	63
NH_2-Lys(Ac)-Asn-DHis-Leu-$CONH_2$, **6**	11.0	8.6	551.60	551.60	90

Anal. gradient: (5-65% B, 30 min)
Prep. gradient: (5-40% B; 25 min)

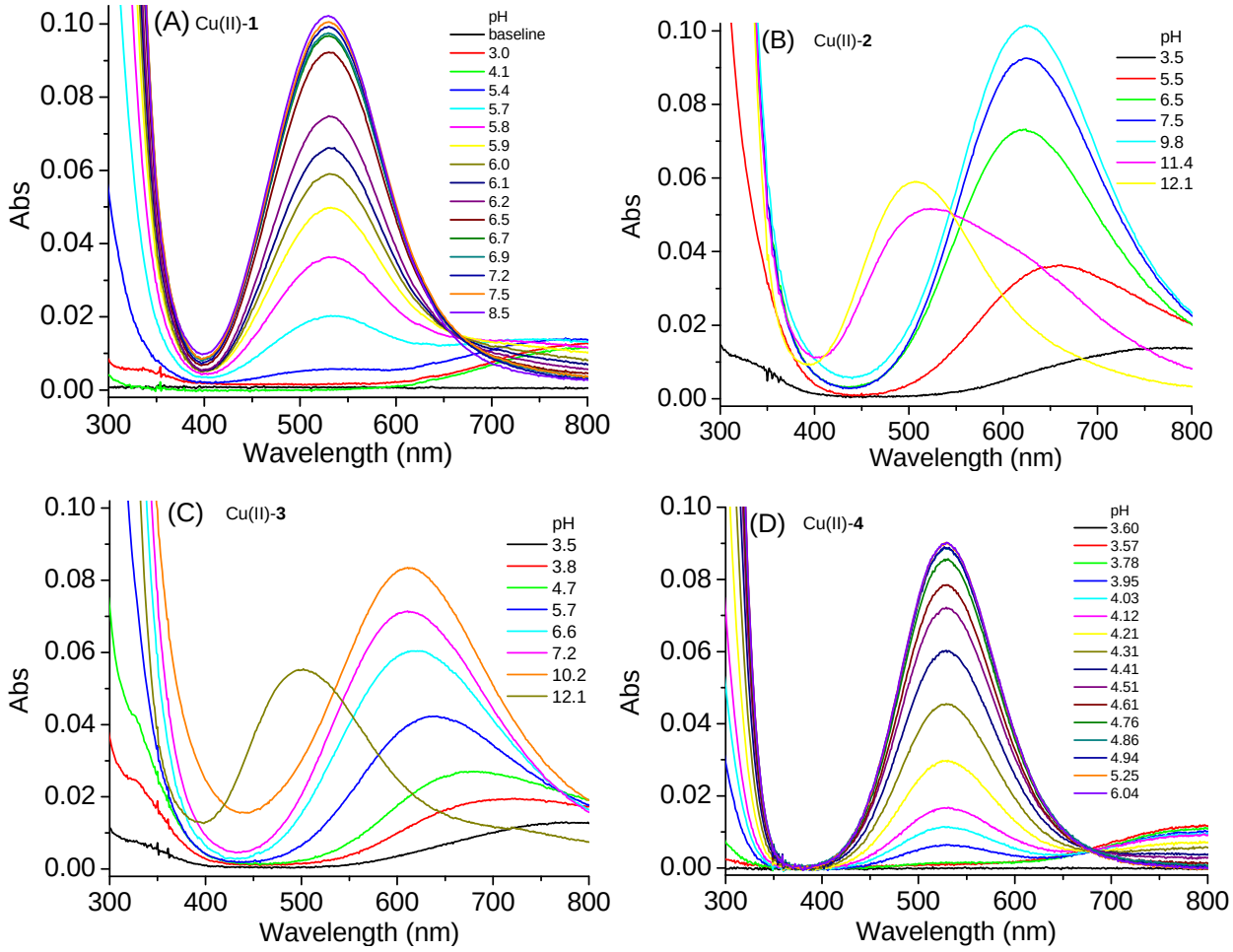

Figure S1. pH dependence of Cu(II) binding to cyclic peptide **1** (A), cyclic peptide **2** (B), cyclic peptide **3** (C) and linear peptide **4** (D). All pH titration experiments were carried out in ultrapure (Barnstead Easypure UF) water and pH was raised with dilute KOH.

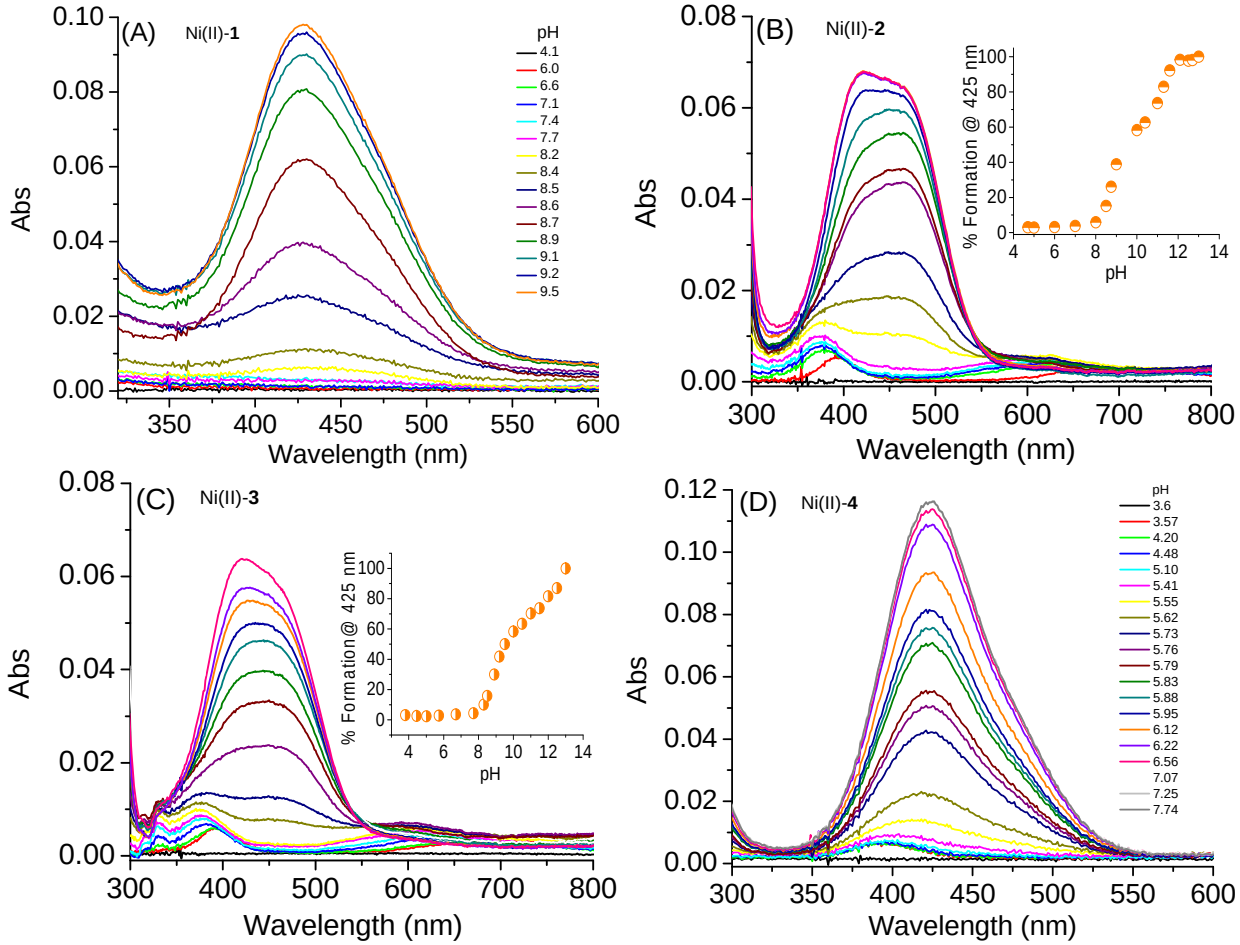

Figure S2. pH dependence of Ni(II) binding to cyclic peptide **1** (A), cyclic peptide **2** (B), cyclic peptide **3** (C) and linear control peptide **4** (D). All pH titration experiments were carried out in ultrapure water and pH was raised with dilute KOH.

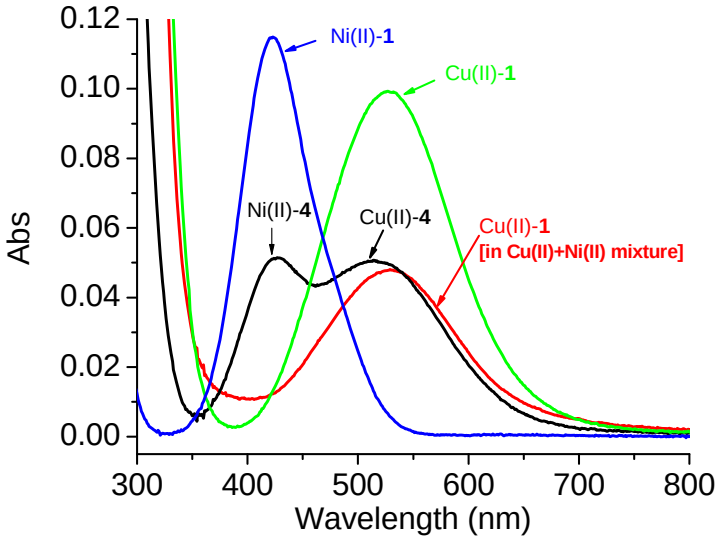

Figure S3. UV-vis spectra of 1 mM Ni(II)-**1** complex (blue), 1 mM Cu(II)-**1** complex (green), and mixtures of 0.5 mM Ni(II) and 0.5 mM Cu(II) with either 1 mM **1** or 1 mM **4** (red and black, respectively). Complexes were prepared at pH 7.5 in N-ethylmorpholine buffer using $CuCl_2$ and $NiCl_2$.

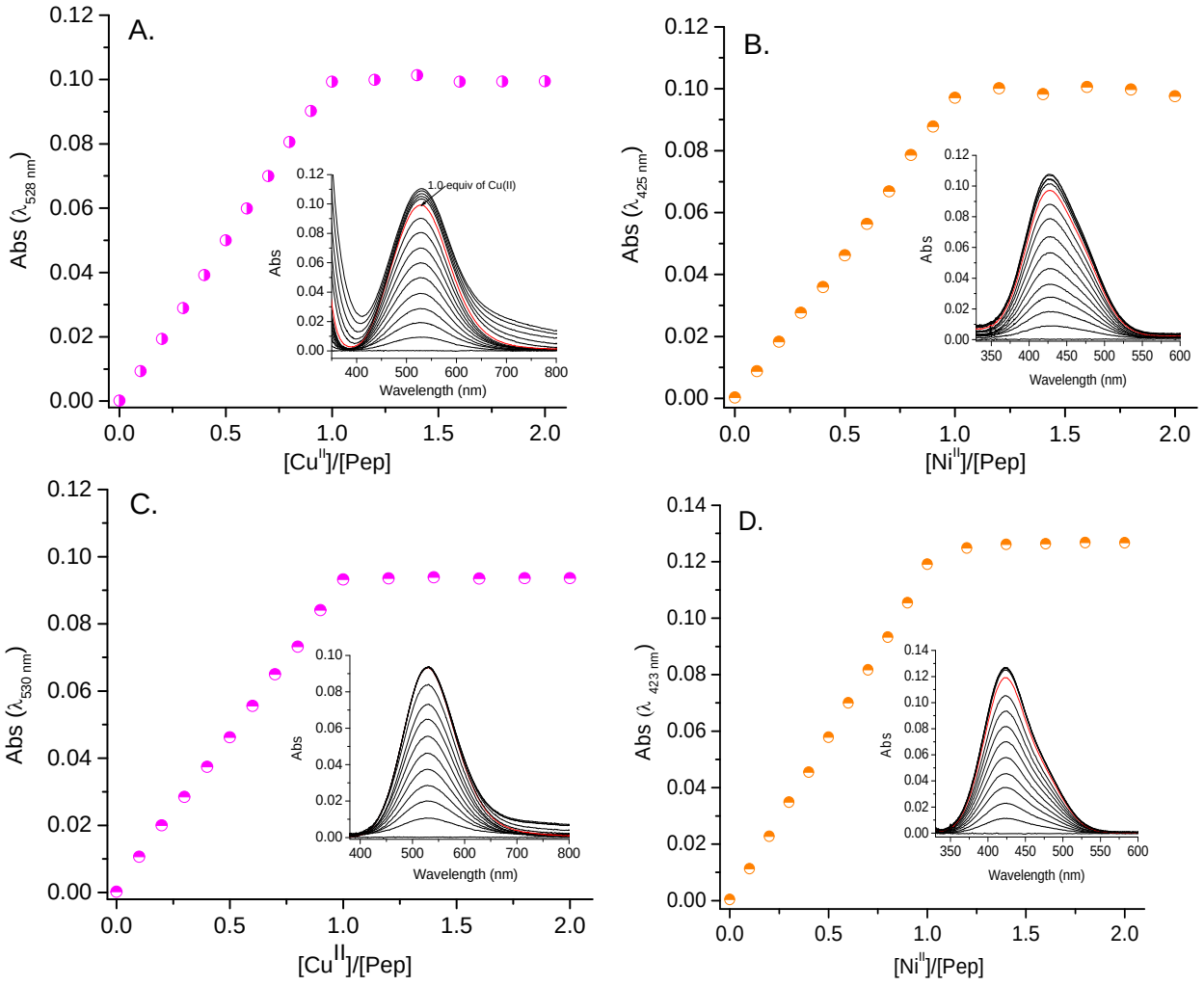

Figure S4. Titration plots showing the UV-vis absorption (*d-d* transition) change during titration with Cu(II) and Ni(II) for cyclic peptide **1** and linear peptide **4**. (A) Cu(II) versus **1** (pH 7.5); (B) Ni(II) versus **1** (pH 9.5); (C) Cu(II) versus **4** (pH 7.5); (D) Ni(II) versus **4** (pH 7.5). Insets show the UV-vis spectra from each titration experiment, with the spectrum at 1:1 ratio shown in color. All titration studies were performed in 50 mM NEM buffer at room temperature.

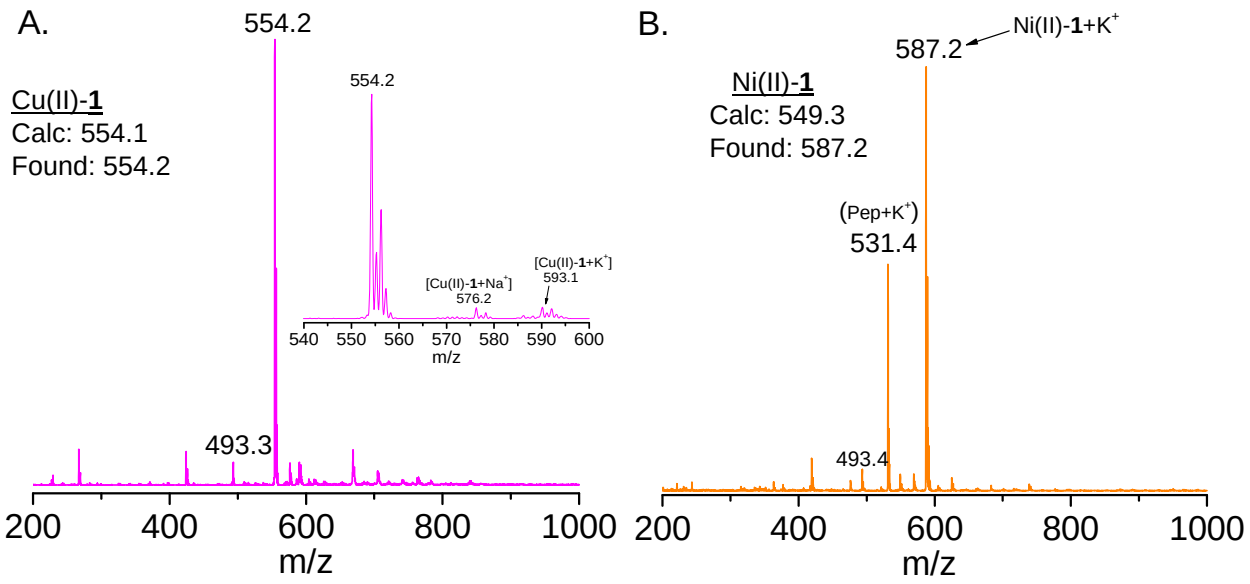

Figure S5. ESI-MS spectra of Cu(II)-**1** (pH 7.5) (A) and Ni(II)-**1** (pH 9.5) (B). The ESI-MS samples (0.1 mM) were prepared in 50 mM NEM buffer with a 1:1.metal:peptide ratio.

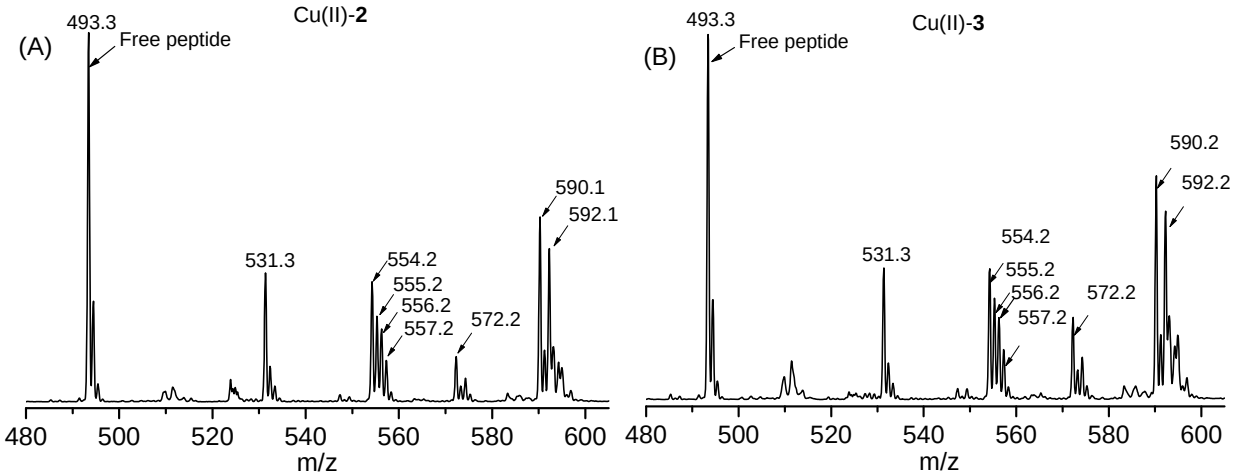

Figure S6. ESI-MS spectra of Cu(II)-**2** (A) and Cu(II)-**3** (B) in NEM buffer (pH 7.5). Masses with an additional 18 and 36 Da are observed, which may be due to the coordination of one or two water molecules to the Cu-peptide complex.

Table S2. ESI-MS data of metallopeptides. All Cu(II)-peptide complexes were prepared in 50 mM NEM buffer (pH 7.5). Ni(II)-peptide complexes were prepared in 50 mM NEM buffer (pH 7.5), except for Ni(II)-**1** for which the pH was 9.5.

Peptides	Metallopeptides			
	Cu(II)-Peptide (M^+)		Ni(II)-peptides (M^+)	
	calc.	found	calc.	found
1	554.1	554.2	549.3	587.2 ($+K^+$)
2	554.1	554.2, 572.2, 590.1	–	–
3	554.1	554.2, 572.2, 590.2	–	–
4	442.9	443.1	438.1	438.1
5	442.9	443.2	438.1	438.0
6	613.1	613.3	608.3	608.3

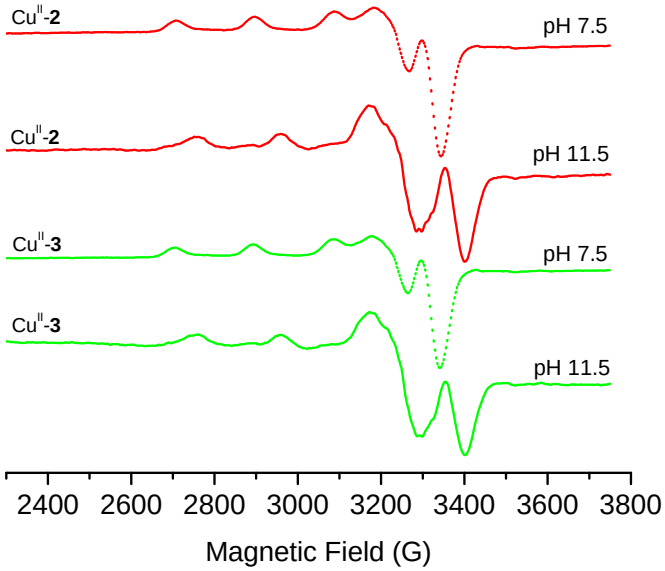

Figure S7. X-band (9.31 GHz) EPR spectra of Cu^{II}-**2** (red) and Cu^{II}-**3** (green) at pH 7.5 and 11.5. All spectra were recorded at 123 K in 100 mM Tris-HCl buffer in presence of 10 % glycerol.

Table S3. EPR properties of Cu(II)-peptide complexes in 100 mM Tris-HCl buffer, pH 7.5 (except where noted), in the presence of 10% glycerol.

Cu^{II}-Peptides	$g_{\perp}$	$A_{\parallel}$ (G)
1	2.046	200
2	2.057 2.050*	187 202*
3	2.057 2.047*	188 202*
4	2.047	198
5	2.048	198
6	2.046	200

* EPR recorded in Tris-HCl buffer, pH=11.5.

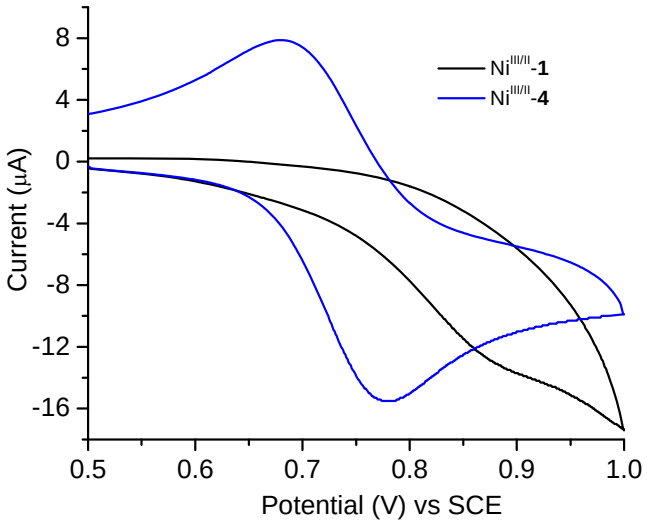

Figure S8. Cyclic voltammograms of Ni(II)-**1** (pH 9.5) and Ni(II)-**4** (pH 7.5) in ultrapure water.

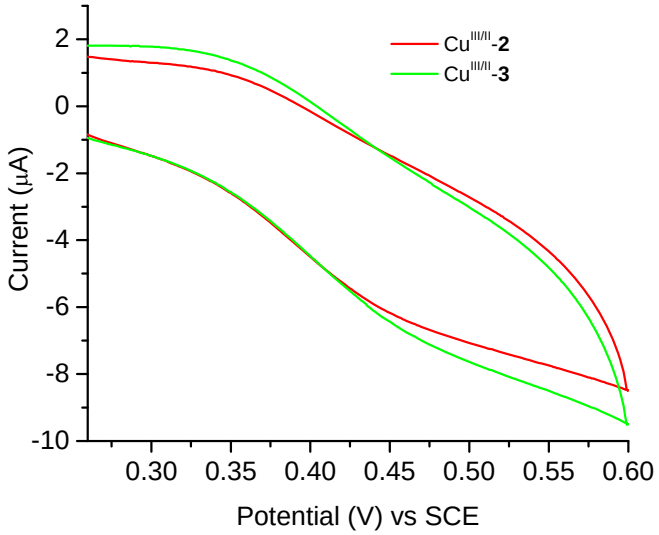

Figure S9. Cyclic voltammograms of Cu(II)-**2** and Cu(II)-**3** in ultrapure water at pH 11.5.

Table S4. Electrochemical data of metallopeptides.

M-Peptide	**E_p^{ox} (V)**	**E_p^{red} (V)**	**ΔE_p (V)**	**$E_{1/2}$ (V)**
Cu(II)-**1**	0.778	0.700	0.078	0.739
Cu(II)-**2**	0.450	0.360	0.090	0.405
Cu(II)-**3**	0.450	0.350	0.100	0.400
Cu(II)-**4**	0.836	0.768	0.068	0.802
Cu(II)-**5**	0.844	0.774	0.070	0.809
Cu(II)-**6**	0.778	0.702	0.076	0.740
Ni(II)-**1**	0.880	Irrev	–	–
Ni(II)-**4**	0.780	0.680	0.100	0.730

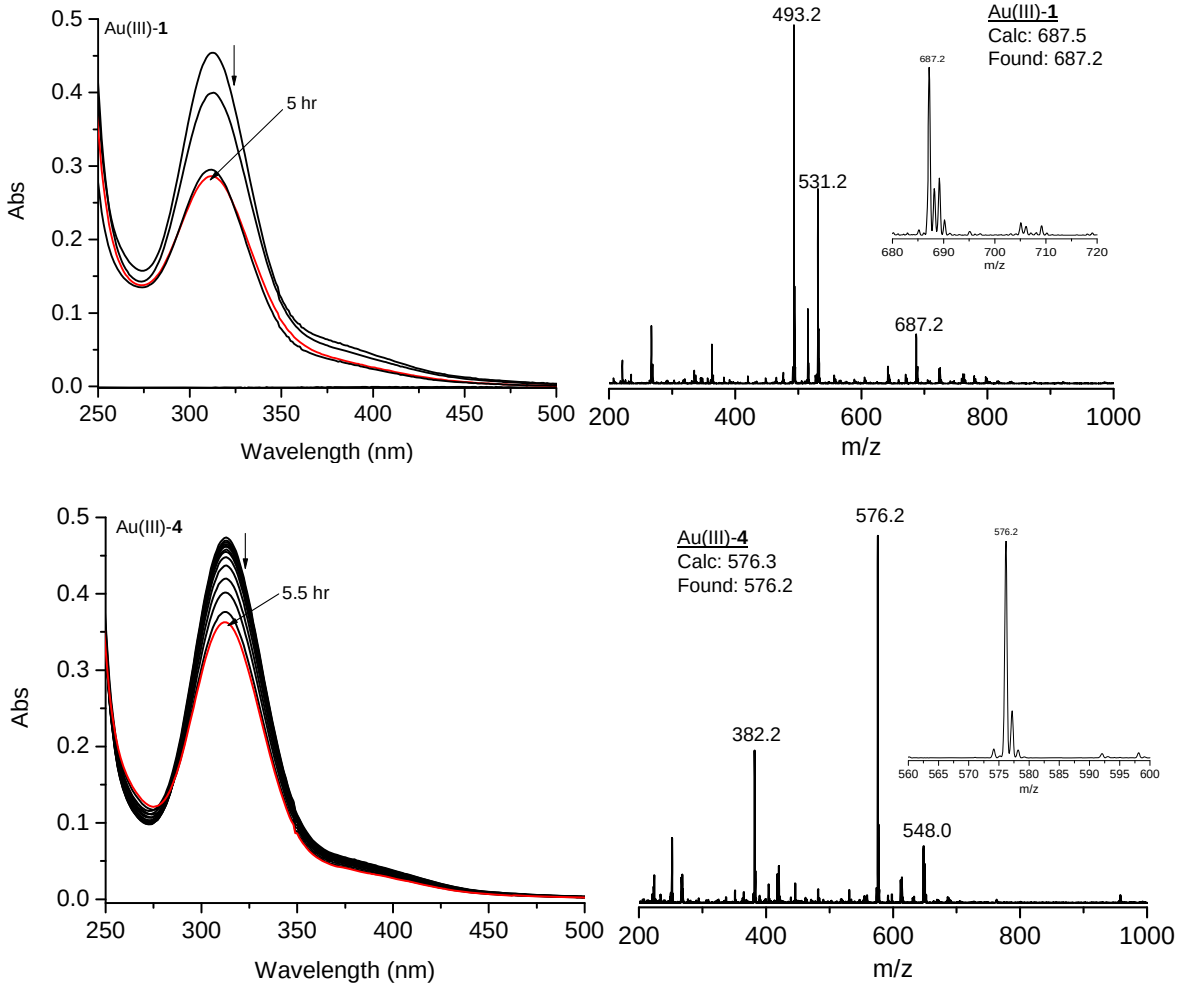

Figure S10. Detection of (a) Au(III) binding to 0.1 mM cyclic peptide **1** and linear peptide **4** by UV-vis (left) and ESI-MS (right). These experiments were performed using 0.1 mM metal cation in ultrapure water with pH adjusted using dilute HCl when necessary.

(a) Pt(II) binding

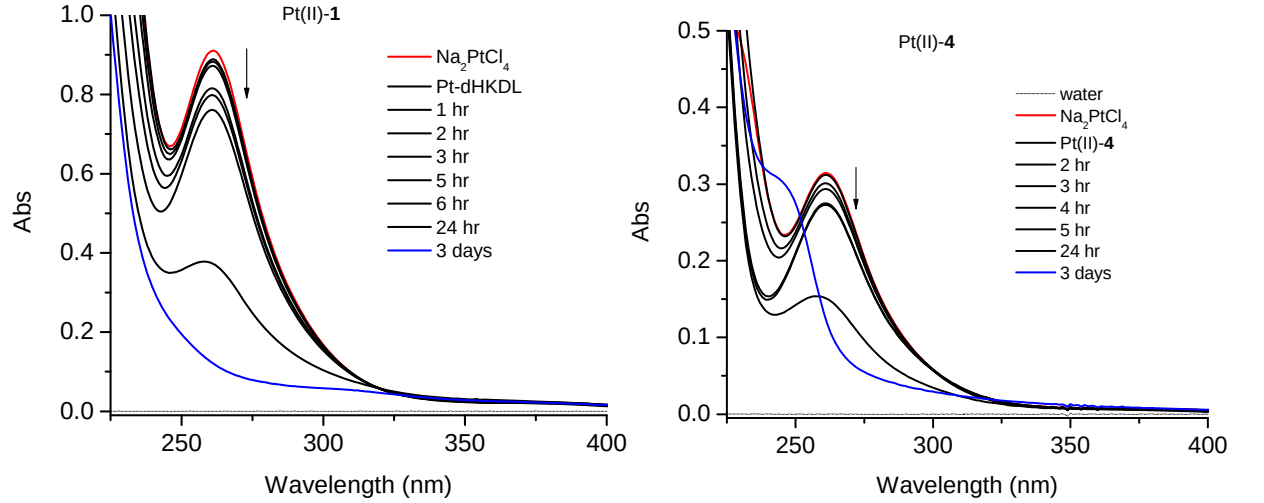

(b) Pd(II) binding

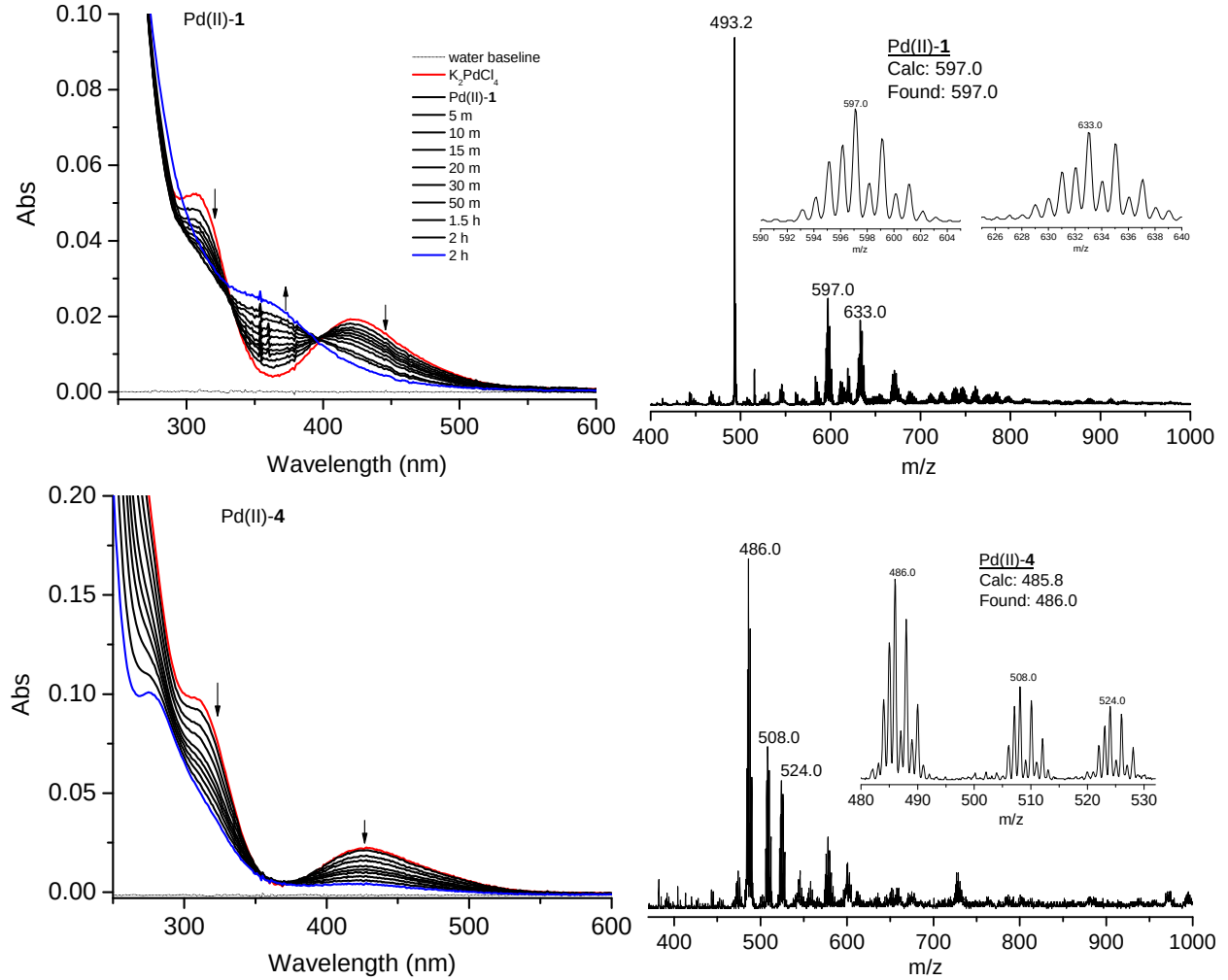

Figure S11. Detection of (a) Pt(II) and (b) Pd(II) binding to 0.1 mM cyclic peptide **1** and linear peptide **4** by UV-vis (left) and ESI-MS (right). These experiments were performed using 0.1 mM metal cation in ultrapure water with pH adjusted using dilute HCl when necessary.